Available online at www.sciencedirect.com
SCIENCE DIRECT
ELSEVIER
Ultramicroscopy 106 (2006) 687–694
ultramicroscopy
www.elsevier.com/locate/ultramic

Effect of cholesterol on the physical properties of pulmonary surfactant films: Atomic force measurements study

Zoya Leonenko[a,*], Eric Finot[b], Vladislav Vassiliev[c], Matthias Amrein[a]

[a]*Department of Cell Biology and Anatomy, Faculty of Medicine, University of Calgary, Calgary, Canada*
[b]*Laboratory of Physics and Nanosciences, Department of Physics, University of Burgundy, Dijon, France*
[c]*Australian National University Supercomputer Facility, Canberra, Australia*

Received 8 October 2005; accepted 10 February 2006

Abstract

Atomic force measurements were performed on supported pulmonary surfactant (PS) films to address the effect of cholesterol on the physical properties of lung surfactant films. We recently found that cholesterol in excess of a physiological proportion abolishes surfactant function, and is the reason that surfactant fails to lower the surface tension upon compression. In this study, we investigated how the loss of mechanical stability observed earlier is related to the local mechanical properties of the film by local force measurements. The presence of 20% of cholesterol in bovine lipid extract surfactant (BLES) resulted in a decrease of the observed adhesive interaction, and an increase in rigidity of the film. We discuss the implication the increased rigidity might have on the functional failure of PS.
© 2006 Elsevier B.V. All rights reserved.

PACS: 61.16.−v; 87.15.−v; 68.60.−p; 68.18.−p

Keywords: Atomic force microscopy; Adhesion forces; Phospholipids; Cholesterol

1. Introduction

Pulmonary surfactant (PS) is a specific mixture of phospholipids and surfactant specific proteins. It forms a molecular film at the interface of the hydrated lung epithelium to the air and thereby reduces the surface tension of the interface to near-zero. This is required for normal respiration and structural stability of the lung.

PS is secreted by the alveolar type II epithelial cells and is composed of phosphatidylcholines (PC, 80% of its mass) with half of the PC being the disaturated dipalmitoylphosphatidylcholine (DPPC). 5–10 mass% is the negatively charged phosphatidylglycerol (PG). Cholesterol is present with 10–20 mol% (5–10% by mass). In addition PS contains two water-soluble (SP-A, SP-D) and two hydrophobic surfactant-associated proteins (SP-B, SP-C), with the latter being permanently associated with the lipids of PS via hydrophobic amino acid side chains. Phospholipids are the primary surface tension lowering components in PS. DPPC is the most abundant molecule and is also the major component in any of the commercial surfactant replacement products. In a pure film, it permits surface tension reduction to near zero values upon compression. In fact, DPPC is the only major component in PS, capable to sustain a film pressure high enough to reduce the surface tensions close to zero in a pure film [1,2]. These properties are very close to the situation found in the lung with respect to the low surface tension achieved, the area reduction required to achieve it and the stability over time [3]. However, DPPC alone is not sufficient to account for the function of PS for several reasons: it adsorbs too slowly to the air–liquid interface to be effective and collapses irreversibly when it is over-compressed or mechanically agitated [4].

The role of a physiological amount of cholesterol has remained unclear, because it does not seem to affect the surface activity. But at an elevated level of cholesterol, 20% by mass, surfactant films fail to reduce surface tension close to zero upon compressions. Such high

*Corresponding author. Tel.: 1 403 210 3809.
E-mail address: zleonenk@ucalgary.ca (Z. Leonenko).

0304-3991/$ - see front matter © 2006 Elsevier B.V. All rights reserved.
doi:10.1016/j.ultramic.2006.02.007

proportion of cholesterol has recently been reported for surfactant, retrieved from acutely injured lungs. These lungs also show a strong decrease in lung compliance, indicating a dysfunctional surfactant. Hence, excess of cholesterol may be the reason for the failure of lung function.

Previous studies [5–9] have demonstrated that, cholesterol plays a key role in controlling the fluidity, permeability, and mechanical strength of lipid membrane. In particular, the incorporation of cholesterol in membrane layers leads to an increased ordering of the hydrocarbon chains of lipids and to a reduction in the area per molecule (partial molar area) for monolayers, the so-called condensation effect [10–14]. In addition, cholesterol broadens and eventually eliminates the liquid-to-solid-phase transition of phospholipid membranes. Phase separation of phospholipids monolayers in the presence of cholesterol has been visualized by atomic force microscopy [15] and showed that lipid monolayer in the presence of cholesterol domains, related to different phases and becomes smooth at high concentration of cholesterol, where the phase separation becomes invisible.

The structure of DPPC and approximate position of cholesterol in relation to lipids is shown schematically in Fig. 1. In the current study, we investigated how the presence of cholesterol influences the local mechanical properties of the film. In order to understand molecular details that could account for the loss of mechanical stability of the cholesterol enriched surfactant failure, we performed local force–distance measurements (force spectroscopy) between the sharp AFM tip (probe) and surfactant films adsorbed to a solid support. Atomic force microscopy is a versatile method to investigate the mechanical properties of lipid films [16–21], and it provides valuable opportunity to relate the forces of sample–probe interactions with the local morphology and microscopic characteristics of the surfaces In force spectroscopy, the AFM probe is moved towards the sample and the interaction force measured as a function of probe sample separation. Attractive and repulsive forces thus observed characterize van der Waals and electrostatic interactions as well as solvation, hydration, and compression- related steric forces [22]. The probe is then retracted from the sample. Upon retraction, the probe may adhere to the sample until it is eventually pulled out of contact. Adhesive interactions include electrostatic, van der Waals, and hydrophobic forces. Force measurements using AFM have been successfully used to analyze mechanical properties and interactions between solid surfaces, [16,23-26] and to address the properties of thin films [27,28] and phospholipids membranes [29–33].

In many particular processes it is fundamentally important to know the adhesive force between particles or between a particle and surfaces, and to find the correlation with the microscopic characteristics of these surfaces, because the adhesive force can characterize the origin of this interactions. The adhesion is not only governed by the nature of the specific interactions between the tip surface and the film. Its magnitude also depends on the size of the contact area. The size of the contact area is defined by the deformation of the two bodies in contact, and the surface forces acting between them. No dependence of the adhesion force on the applied load or the contact time is expected for purely elastic deformations between solid materials [23,24]. But if one of the materials shows visco-elastic deformation, the contact area and adhesion force will increase with contact time [34]. When plastic deformations occur, the adhesion depends on the applied load [34,35]. Therefore the dependence of adhesion on the applied load and load rate reveals information on the contact mechanism and the mechanical properties of the materials involved.

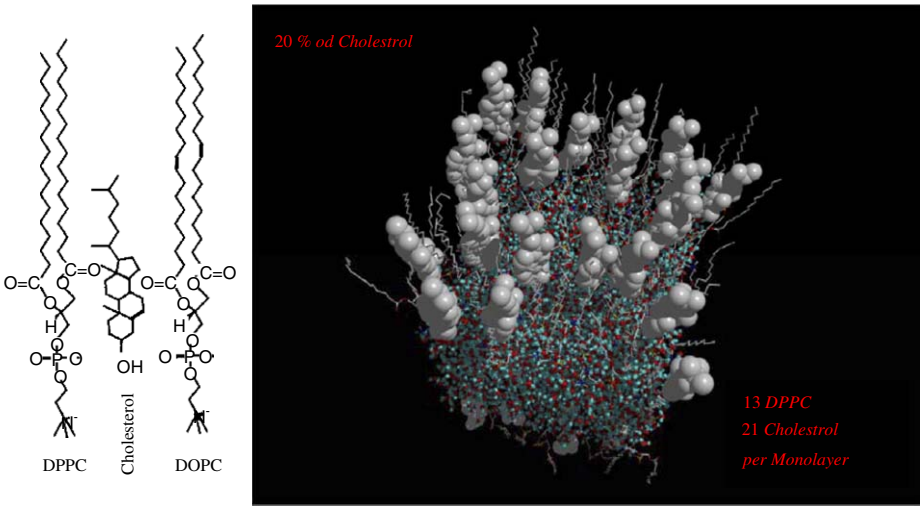

Fig. 1. The structure of saturated and disaturated dipalmitoylphosphatidylcholine DPPC and DOPC lipid molecules and cholesterol and a snapshot of MD simulations showing distribution of cholesterol molecules in DPPC monolayer, corresponding to 20% of cholesterol, cholesterol molecules area shown as balls and lipids as sticks, graphical representation MMPRO. http://sf.anu.edu.au/~vvv900/MMPRO.

2. Materials and methods

BLES is a hydrophobic extract of bovine lung lavage that differs from natural surfactant in the lack of surfactant specific proteins SP-A and SP–D and cholesterol. Phosphatidylcholines (PC) represent 80% of its mass with half of the PC being the disaturated dipalmitoylphosphatidylcholine (DPPC). 5–10 mass% is the negatively charged phosphatidylglycerol (PG), and two hydrophobic surfactant-associated proteins (SP-B, SP-C). BLES in non-buffered normal saline (pH 5-6) with a phospholipid concentration of 27 mg/ml was a kind gift by the manufacturer (BLES Biochemical Inc. of London, Ontario). Cholesterol was purchased from Sigma Chemicals, St. Louis, MO. A solution of 1:1:1 ratio of methanol, chloroform, and BLES by volume was first vortexed and then spun at 100 *g* for 5 min. The methanol/water phase was discarded and the BLES in chloroform was retained and either 5 or 20% of cholesterol (by mass) with respect to phospholipids in chloroform was added. Each solution was then dried under N_2 and resuspended with Goerke's buffer (140 mM NaCl, 10mM Hepes and 2.5mM CaCl2; pH 6.9) to obtain an aqueous suspension of BLES and cholesterol at a concentration of 27 mg/ml phospholipids.

BLES solutions were spread at the air liquid interface with Goerke's buffer as a subphase. Supported planar monolayers on mica were prepared using Langmuir–Blodgett technique and transferred on mica support when films were compressed at surface tension 25 mN/m (compression 47mN/m). Supported films were imaged in air using NanoWizard AFM from JPK Instruments, Germany.

The atomic force microscope was also used as a force apparatus. We performed force measurements on BLES films. The experiment consisted in monitoring the interaction between the AFM tip and the sample surface at monolayer and multilayer areas by sensing the cantilever deflection as a function of the piezo elongation, as the tip was moved toward and away from the substrate. In an AFM force measurement, the probe is moved towards the sample and the cantilever deflection Z_c is measured as a function of the distance between the scanner and the sample Z_p. A statistical analysis [31] has revealed that 10 measurements (force curves) at different locations of the same area are required to determine adhesion with 10% accuracy. As the tip-sample separation cannot be independently measured, we used systematic procedure for calculating the sensitivity of the apparatus, described in [31]. Raw data (Z_c versus Z_p) are then converted into force F versus surface–tip separation D using Hooke's law, as described in Ref. [16].

It is a well-known fact that the force interactions depend on the velocity of the surface approach [16], especially for soft viscoelastic materials. All measurements were performed at 25 °C, over five different velocities, collecting each time 10 force curves. Silicon cantilevers from Micromash, Spain, were used with cantilever spring constant 0.6 and 0.7 N/m as determined by thermo-fluctuation method using JPK SPM software. Forces were measured on several different structural areas of the film, by positioning the AFM tip after the image was collected.

3. Results and discussion

Here we present force measurement on such BLES films with 5% and 20% of cholesterol to elucidate the effect of cholesterol. As the function and morphology of BLES with 0% and 5% cholesterol are the same we measured the forces on BLES films with 5% cholesterol, which is a physiological amount of cholesterol. Fig. 2 shows compression versus surface area isotherm.

The area to the right of the plateau corresponds to lower compression and relaxed monolayer. We have shown earlier that the plateau in the isotherm is due to the formation of lipid double-layer structures adjacent to a molecular monolayer at the interface [36,37]. We collected samples of the film after compression beyond the the plateau region of the isotherm (pressure 47 mN/m).

Typical areas where force curves were collected are shown in Fig. 3. For BLES with 20% cholesterol only monolayer was present and chosen for force measurements. The image cross-section analysis shows that the height of the multilayer area at point 2 is 4.5 nm, which corresponds to the height of a bilayer attached to the surface of monolayer. The monolayer thickness is typically 2–2.5 nm. We performed force measurements both, on monolayer areas and on a first bilayer adjacent to the monolayer. Typical raw data plots are shown in Fig. 4.

At the beginning of the force curve measurement, the cantilever is far away from the sample. Approach part of the curve starts with the largest height measured on the x-axis (right). This corresponds to horizontal part of the curve, which continues until cantilever comes into close proximity of the sample. At the contact point, the cantilever starts to deflect and the repulsive force rises upon

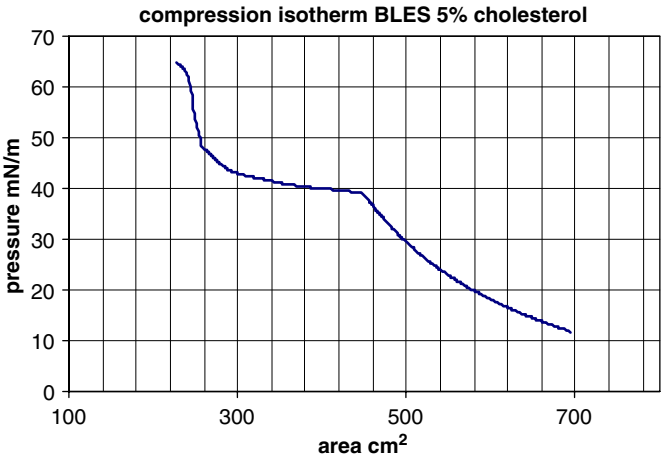

Fig. 2. Surface pressure versus surface area isotherm collected during compression of BLES film spread from Goerke's buffer onto Goerke's buffer subphase, after this BLES film was supported on mica at compression 47 mN/m.

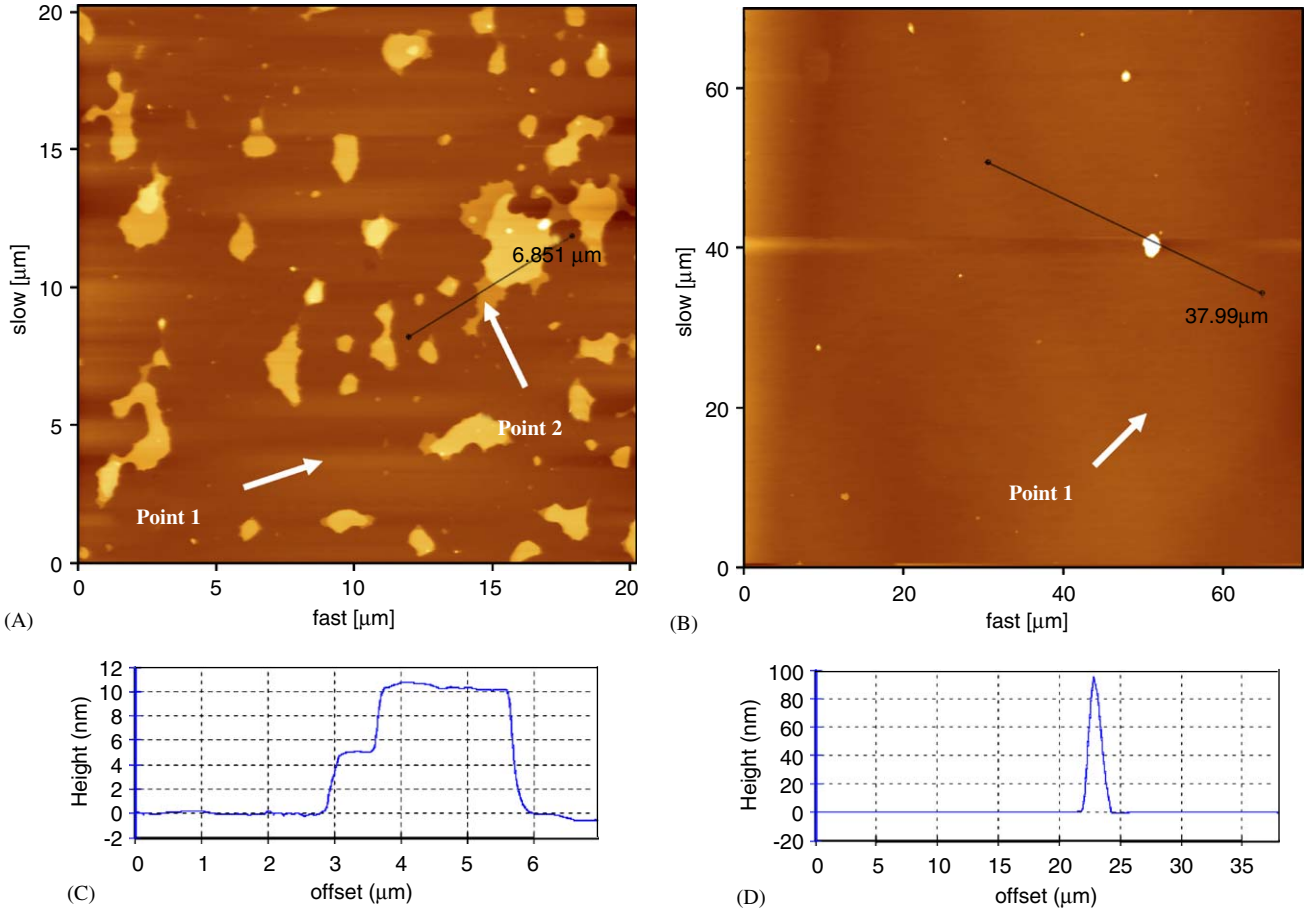

Fig. 3. (A) BLES supported film with 5% cholesterol, with the typical points where forces were measured on monolayer—point 1, and bilayer—point 2; (B) BLES with 20% cholesterol only monolayer was present and chosen for force measurements; the lower part shows cross-section across the images.

further approaching the cantilever base to the sample, showing a progressive increase in vertical deflection. After this, the scanner is moved backwards and the cantilever is retracted from the sample surface. The retraction (or retrace) part corresponds to the decrease in vertical deflection, until the cantilever comes out of contact and after this the curve becomes horizontal again. The return part of the curve, retraces the approach part for mica. But this is not the case for pulmonary surfactant films. The retraction part of the curve extends beyond the horizontal level of the x-axis due to adhesion between the sample surface and the AFM tip.

The largest adhesion was measured at the BLES multilayer structure, (which corresponds to the point 2, Fig. 3A)

To analyze adhesive forces we employed the statistical analysis described in Ref. [31]. Briefly, the force of a unit interaction between an AFM tip and a surface is determined from a statistical analysis of a series of detachment force measurements. For a statistical analysis based on adhesive force originating from a discrete number n of individual interactions or bonds, F_s have been used. The total force distribution follows Poisson statistics, where both the adhesion force F_{adh} and the variance σ originates from a number of individual bonds n.

$$F_{adh} = n\,F_s \text{ and } \sigma^2 = n\,F_s^2.$$

The force of one bond, F_s, is therefore given by the square of the variance of the force divided by the mean adhesion force F_{adh}. The value n is the ratio between F_{adh} and F_s. This analysis has the advantage that the knowledge of the mean radius of curvature is not required [38] and gives information on the nature of the film. Table 1 presents the standard deviation of the adhesion force measured on BLES monolayer and bilayer. This analysis allows one to correlate microscale changes of the physical properties of the film with molecular structure and mobility of individual lipid molecules. Tails mobility can be seen as the number of molecules n in contact with the AFM probe. The larger n is, the higher the mobility. The change in mobility increases the number of bonding n and therefore F_{adh} and σ.

BLES with 5% cholesterol at the bilayer area has an adhesion of 60 nN, which is higher than the monolayer. BLES with 20% cholesterol has a lower adhesion than BLES monolayer with 5% cholesterol. It is interesting that "single force" F_s was slightly lower in the presence of 20% cholesterol, 3 nN compared to 4 nN with 5% cholesterol

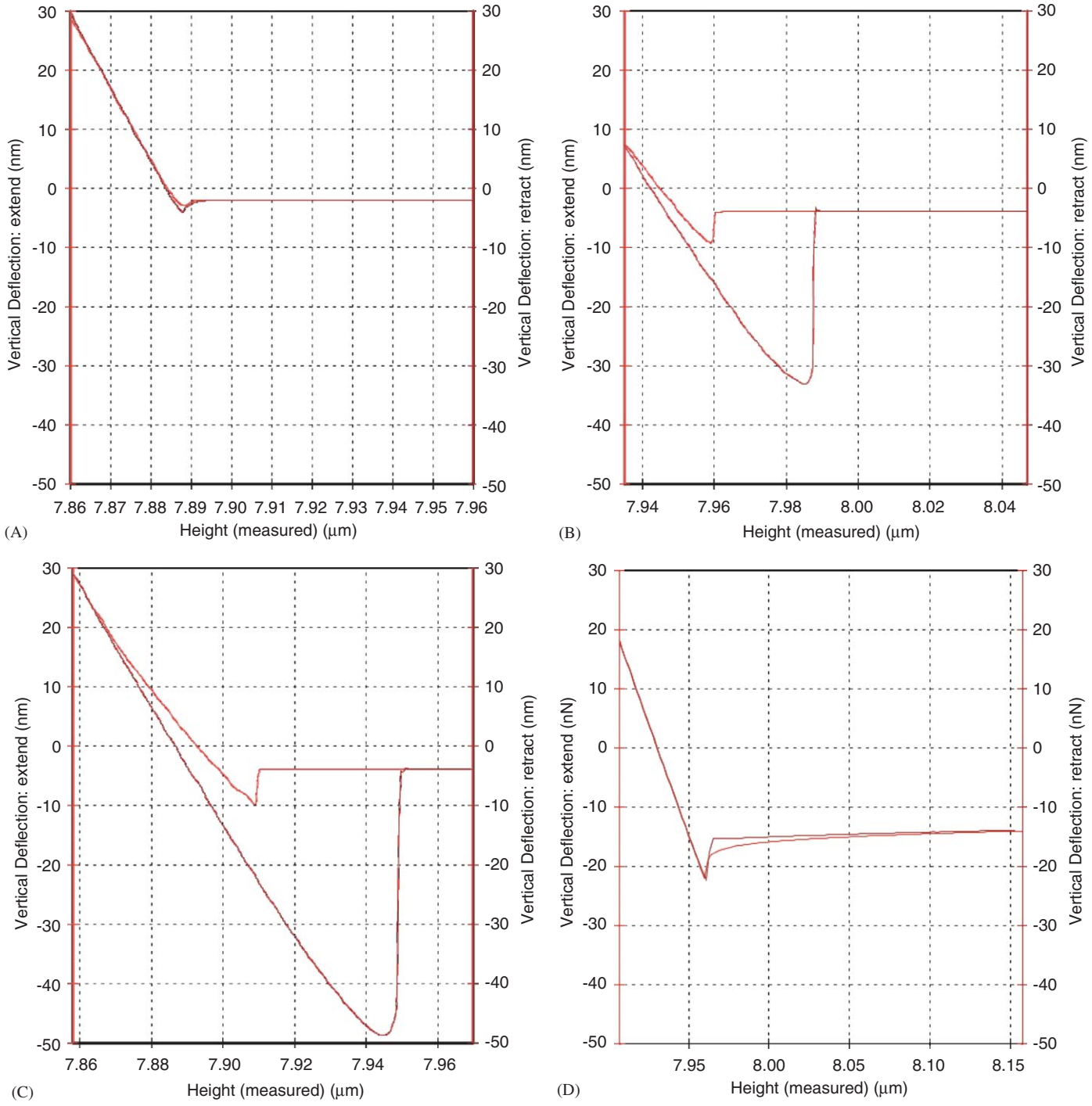

Fig. 4. (A) typical force curve on mica, (B) on BLES supported film with 5% cholesterol at the monolayer area, point 1; (C) on BLES supported film with 5% cholesterol at the multilayer area, point 2; (D) on BLES supported film with 20% cholesterol at the monolayer area, point 1.

but the number of bonds decreased significantly from 15 and 10 to 7 (Table 1). Therefore the presence of 20% of cholesterol decreases fluidity of the monolayer.

The increase in the adhesive force for a bilayer as compared to a monolayer may be understood by an increase in contact area of probe and sample at a given load. This is because the tip may now penetrate the sample deeper due to the increase in thickness of the compliant surfactant matter between the hard mica support and probe. An increased compliance in good agreement with the Hertz model for describing the indentation of the probe in the sample with increased height of multi-lamellar lipid stacks has been found by us earlier [39,40].

BLES with 20% cholesterol reveals the smallest adhesion force, compared to monolayer and multilayer areas of BLES with 5% cholesterol. This indicates that adhesive properties of the film were considerably altered by the incorporation of 20% cholesterol. The lipid molecules are

not mobile enough in the presence of 20% cholesterol and cannot be easily rearranged around the tip to increase the contact area and adhesion force.

The parameters, which can also influence adhesion, are the rate of the approach of the probe and the maximum force applied to the sample. The adhesion between surfaces is governed by the deformation of the two bodies in contact, and the surface forces acting between them. No dependence of the adhesion force on the applied load or the contact time is expected in the DMT [24] and JKR [23] models, developed for solid materials, where deformations remain purely elastic. If one of the materials shows viscoelastic deformation, the contact area and adhesion force will increase over time [34]. When plastic deformations occur, the adhesion depends on the applied load [34,35]. Therefore the dependence of adhesion on the applied load and load rate can reveal much about the contact mechanics and the mechanical properties of the materials involved.

In the current study, the adhesion forces increased exponentially with a lower rate (i.e. longer the contact time) for all samples investigated (Fig. 5). This finding is similar to observations made with polymer films [41], and lipid membranes [31]. For the surfactant films studied here, the rate dependant rupture force most likely reflects the lateral mobility and/or the packing density of the lipids. A higher mobility of the lipid molecules should produce a larger change of the contact area over time, as the molecules can arrange themselves around the AFM tip. The contact area between the tip and the sample can be related to adhesion force and Young's modulus as in Ref. [16]:

$$a = \left(\frac{RF_{\mathrm{adh}}}{E}\right)^{2/3},$$

Therefore, the increase in contact area will produce the increase in adhesion force, which is well confirmed by experimental data. For BLES with 5% cholesterol the slope is steeper (Fig. 5) than for films containing 20% cholesterol. This indicates that the lipids are more mobile and the film more viscous for films containing 5% as compared 20% cholesterol.

Only a small variation of adhesion was found for all samples with the maximum loading force varied over three orders of magnitude. No variation was found on pure mica.

Cholesterol is a membrane-active molecule, and by interacting with phospholipids it modulates the conformation of the phospholipids acyl chains [42–45]. It orients in a phospholipid bilayer with its polar head group in the aqueous phase and its hydrophobic chains parallel with the adjacent phospholipid molecules, Fig. 1. It has been reported earlier [46] that cholesterol has a dual effect on membrane fluidity. At temperatures below the phospholipid phase transition temperature, cholesterol molecules interfere with the tight packing of the phospholipids molecules that is required for gel formation, giving rise to a fluidizing effect. An opposite effect is observed at temperatures above the phase transition temperature of the phospholipids. The incorporation of cholesterol in membrane layers leads to an increased ordering of the hydrocarbon chains of lipids and to a reduction in the molecular area for monolayers, the so-called condensation

Table 1
Experimental adhesion force F_{adh} and its standard error sigma on BLES bilayer, monolayer with 5% cholesterol and BLES monolayer with 20% cholesterol, measured at room temperature

	BLES 20% cholesterol monolayer	BLES 5% cholesterol monolayer	BLES 5% cholesterol bilayer
F_{adh}	20 nN	40 nN	60 nN
sigma	8 nN	12 nN	15 nN
F_{s}	3 nN	4 nN	4 nN
n	7	10	15

Calculation of the number of bindings n and the mean force of a single bond F_{s} Rate = 200 nm/s, load = 20nN. Adhesion force on pure mica, does not exceed 1.5 nN.

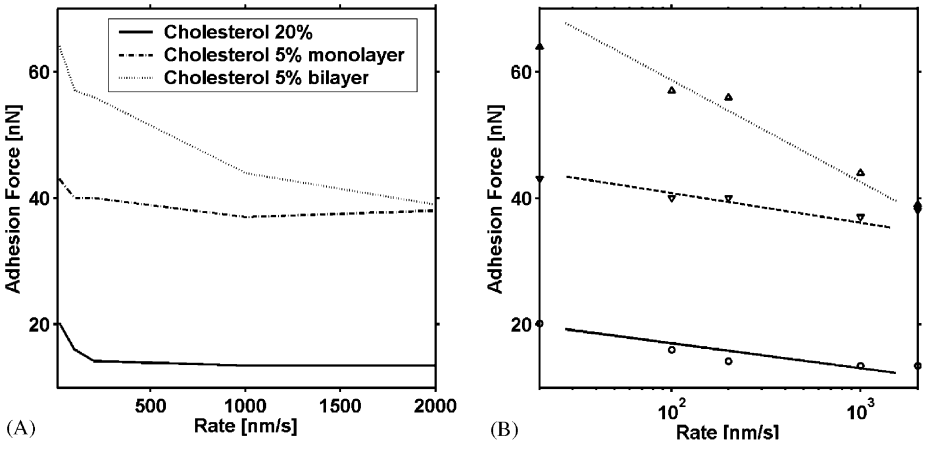

Fig. 5. Adhesion force versus rate of retraction on a linear (A) and logarithmic rate scale (B).

effect. On a larger scale, cholesterol broadens and eventually eliminates the liquid-to-solid-phase transition of phospholipid membranes [5-8]. On a smaller scale, molecular dynamics simulations reported the condensing effect of cholesterol observed in mixed cholesterol–lipid bilayer systems [47,48]. Experimental studies of mixed monolayers of phospholipid/cholesterol at the air/water interface also indicated that cholesterol has a pronounced condensing effect for monolayers [49–51]. On the basis of phospholipid/cholesterol monolayer studies, this condensing effect reduces the number of defects and increases the packing density of the monolayer.

Considering the dual effect of cholesterol in a surfactant layer, two aspects are likely important in the context of this study. In the fluorescence light microscope studies of phase separated films of saturated and unsaturated lipid monolayers, cholesterol has been shown to segregate into the already condensed phase of the saturated lipids [14,47]. Secondly, at equilibrium surface tension, the phase separation is no longer apparent in a light microscope. Likely, in analogy to lipid rafts, cholesterol disperses homogenously within the film together with DPPC in entities, too small to be visible in a conventional light microscope. Hence, at a physiological proportion, cholesterol may mainly interact with DPPC and make these domains small in size and slightly more fluid. In accordance with this view, our results on BLES surfactant films show that when 5% cholesterol is present in BLES surfactant film we observe high fluidity of the layer. This molecular arrangement is able to withstand high later film pressure without collapse.

On the other, at a patho-physiological high proportion of cholesterol, an excess of cholesterol may now be forced to interact with the fluid phase lipids and make these areas of the film more rigid, in accordance with our observation by the force measurements. The increase in rigidity and decrease in adhesion forces that we observed in our experiments in the presence of 20% cholesterol also correlate well with earlier reported results that the presence of 10-30 mol % cholesterol mixed monolayers strongly suppressed protein adsorption due to highly packed phosphocholine groups [52]. This molecular configuration is no longer able to withstand a high lateral pressure and collapses [53].

4. Conclusions

In this work with atomic force measurements we have shown that the presence of 20% of cholesterol, significantly alter physical properties of the BLES surfactant films, decreasing adhesive interaction, and increasing the rigidity of the film. The increased rigidity of the film and decreased adhesion that we observed may play an important role for understanding the interaction of surfactant films with each other, proteins and inorganic structures.

Acknowledgements

This work was supported by CIHR. Authors acknowledge the help of Jana Döner and Lasantha Gunasekara for preparing the samples, and Dr. Elmar Prenner for letting us use the Langmuir-Blodgett trough, and Dr. Christian Le Grimellec for helpful discussions during conference presentation.

References

[1] A.D. Bangham, C.J. Morley, M.C. Phillips, Biochim. Biophys. Acta 573 (1979) 552.
[2] M. Amrein, D. Knebel, M. Haufs, in: Molecular Mechanisms in Lung Surfactant (Dys) Function, Lung Biology Series, Marcel Dekker Inc., NY, 2005.
[3] S. Schurch, Respir. Physiol. 48 (1982) 339.
[4] S. Schurch, F.H. Green, H. Bachofen, Biochim. Biophys. Acta 1408 (1998) 180.
[5] R.A. Demel, B.D. Kruyff, Biochim. Biophys. Acta 457 (1976) 109.
[6] H. Ohvo-Rekilä, B. Ramstedt, P. Leppimäki, J.P. Slotte, Prog.Lipid Res. 41 (2002) 66.
[7] T.P. W McMullen, R.N.A. Lewis, R.N. McElhaney, Curr. Opin. Colloid Interface Sci. 8 (2004) 459.
[8] M. Bonn, S. Roke, O. Berg, L.B.F. Juurlink, A. Stamouli, M. Muller, J. Phys. Chem. B 108 (2004) 19083.
[9] G.A. Cadenhead (Ed.), Structure and Properties of Cell Membranes, CRC Press, Boca Raton, FL, 1985.
[10] V.T. Moy, D.J. Keller, H.E. Gaub, H.M. McConnell, J. Phys.Chem. 90 (1986) 3198.
[11] R.M. Weis, H.M. McConnell, J. Phys.Chem. 89 (1985) 4453.
[12] S. Subramaniam, H.M. McConnell, J. Phys.Chem. 91 (1987) 1715.
[13] J.P. Slotte, Biochim. Biophys. Acta 1238 (1995) 118.
[14] L. A .Worthman, K. Nag, P.J. Davis, K.M. Keough, Biophys. J. 72 (1997) 2569.
[15] C. Yan, L. Johnston, J. Micros. 205 (2002) 136.
[16] B. Cappella, G. Dietler, Surf. Sci. Reports 34 (1999) 1.
[17] A. Janshoff, M. Neitzert, Y. Oberdörfer, H. Fuchs, Angew. Chem. Int. Ed. 39 (2000) 3212.
[18] H. Mueller, H.J. Butt, E. Bamberg, Biophys J. 76 (1999) 1072.
[19] L.O. Heim, S. Ecke, M. Preuss, H.J. Butt, J. Adhes. Sci. Technol. 16 (2002) 829.
[20] Y.F. Dufrene, T. Boland, J.W. Schneider, W.R. Barger, G.U. Lee, Faraday Discuss 111 (1998) 79.
[21] A. Ikai, R. Afrin, Cell Biochem. Biophys. 39 (2003) 257.
[22] G. Binnig, C.F. Quate, C. Gerber, Phys. Rev. Lett 56 (1986) 930.
[23] K.L. Johnson, K. Kendall, A.D. Roberts, Proc. R. Soc. London A 324 (1971) 301.
[24] B.V. Derjaguin, V.M. Muller, Yu.P. Toporov, J. Colloid Interface Sci. A 53 (1975) 314.
[25] H. Hertz, J. Reine, Angew. Mathematik. 92 (1882) 156.
[26] D. Maugis, J. Colloid Interface Sci. 150 (1992) 243.
[27] E.W. van der Vegte, G. Hadziioannou, Langmuir 13 (1997) 4357.
[28] E.K. Dimitriadis, F. Horkay, J. Maresca, B. Kachar, R.S. Chadwick, Biophys. J. 82 (2002) 2798.
[29] V. Franz, S. Loi, H. Muller, E. Bamberg, H.-J. Butt, Coll. Surf. B Biointerface. 23 (2002) 191.
[30] S. Loi, G. Sun, V. Franz, H.-J. Butt, Phys. Rev. E. 66 (2002) 031602.
[31] Z.V. Leonenko, E. Finot, H. Ma, T.E.S. Dahms, D.T. Cramb, Biophys. J. 86 (2004) 3783.
[32] R. Afrin, T. Yamada, A. Ikai, Ultramicroscopy 100 (2004) 187.
[33] P.E. Milhiet, V. Vie, M.C. Gioconde, C. Le Grimellec, Single molecules 2 (2001) 109.
[34] M. Kappl, H.J. Butt, Part. Part. Syst. Charact. 19 (2002) 129.
[35] D. Maugis, H.M. Pollock, Acta Metall 32 (1984) 1323.

[36] D. Knebel, M. Sieber, R. Reichelt, H.J. Galla, M. Amrein, Biophys. J. 82 (2002) 474.
[37] A. von Nahmen, M. Schenk, M. Amrein, Biophys. J. 72 (1997) 463.
[38] J.M. Williams, T. Han, T.P. Beebe Jr., Langmuir 12 (1996) 1291.
[39] M. Schenk, M. Amrein, R. Reichelt, Ultramicroscopy 65 (1996) 1.
[40] M. Amrein, M. Schenk, A. Vonnahmen, J. Microscopy 179 (1995) 261.A.
[41] G. Sun, M. Kappl, H.-J. Butt, Europ. Polym. J. 41 (2005) 663.
[42] G.A. Cadenhead, Structure and Properties of Cell Membranes, vol. III, CRC Press, Boca Raton, FL, 1985.
[43] E. Oldfield, D. Chapman, Biochem. Biophys. Res.Commun. 43 (1971) 610.
[44] D. Chapman, N.F. Owens, M.C. Phillip, D.A. Walker, Biochim. Biophys. Acta 183 (1969) 458.
[45] M.R. Vist, J.H. Davis, Biochemistry 29 (1990) 451.
[46] B.M. Discher, K.M. Maloney, D.W. Grainger, S.B. Hall, Biophys. Chem. 333 (2002) 101–102.
[47] C. Hofsäß, E. Lindahl, O. Edholm, Biophys. J. 84 (2003) 2192.
[48] A.M. Smondyrev, M. Berkovitz, Biophys. J. 77 (1999) 2075.
[49] J.P. Slotte, Biochemistry 31 (1992) 5472.
[50] P. Mattjus, R. Bittman, J.P. Slotte, Langmuir 12 (1996) 1284.
[51] D.W. Lynn-Ann, N. Kaushik, J.D. Philip, M.W.K. Kevin, Biophys. J. 72 (1997) 2569.
[52] K. Kim, C. Kim, Y. Byun, Langmuir 17 (2001) 5066.
[53] L. Gunasekara, M. Shoel, S. Schurch, Z. Leonenko, K. Nag, M. Haufs, M. Amrein, Biophys. Biochim. Acta 27 (2005) 2737.

Further reading

[54] M.M. Lipp, K.Y.C. Lee, D.Y. Takamoto, J.A. Zasadzinski, A.J. Waring, Phys.Rev.Lett. 81 (1998) 1650.